

## Molecular dynamics studies of $\text{ZnAl}_2\text{O}_4$ spinel

Luis Javier Alvarez <sup>a</sup>, Pedro Bosch <sup>b</sup> and Miguel Angel Valenzuela <sup>b,c</sup>

<sup>a</sup> *Dirección General de Servicios de Cómputo Académico,  
Universidad Nacional Autónoma de México, Circuito Exterior,  
Ciudad Universitaria México, 04510 Mexico, DF Mexico*

<sup>b</sup> *Departamento de Química, Universidad Autónoma Metropolitana-Iztapalapa,  
Av Michoacán y Purísima, Iztapalapa 09340 Mexico, DF Mexico*

<sup>c</sup> *Instituto Mexicano del Petróleo, Eje Lázaro Cárdenas 152, CP 07730 Mexico, DF Mexico*

Received 18 March 1993; accepted 7 August 1993

Molecular dynamics simulations of  $\text{ZnAl}_2\text{O}_4$  spinel have been carried out at 300 and 800 K. Comparison with experimental data shows that at low temperature the most favorable configuration is that of a mixed spinel. As temperature increases the structural transformation becomes more evident. A detailed interpretation of the experimental vibrational spectrum and radial distribution functions is obtained.

**Keywords:** Molecular dynamics;  $\text{ZnAl}_2\text{O}_4$ ; spinel structure; XRD; IR

### 1. Introduction

Studies on metal supported catalysts are often focused only on the analysis of the metallic particles before or after the reaction. However, metal supported catalysts are dynamical systems where sintering or any other structural evolution has to be followed. This evolution depends not only on the metal phase but also on the support [1].

Supports, during the reaction, have to be stable and have to maintain the necessary surface area as well as an adequate porosity. Although supports are often considered as simple diluents, they may alter the metal performance (metal-support interaction) or simply act as a catalyst (bifunctional catalysts) [2].

Porous refractory solids, as zinc aluminate, have been shown experimentally to present the features required of a support [3]. Furthermore, the surface area of zinc aluminate may be experimentally controlled by doping the spinel with calcium [4]. To understand these kinds of structural modifications in spinels, much has been done in recent years. In the field of theoretical chemistry, a quantum chemical method to calculate the structure preference energies for normal or inverse spinels has been developed [5]. This method uses normalized cation and anion two-body

repulsion energies and can be successfully compared with the crystal field and classical potential methods. Through molecular-dynamics simulations, the structure and dynamics of  $\gamma$ -Al<sub>2</sub>O<sub>3</sub> (defectuous spinel) have been reinterpreted using pairwise additive interaction potentials of Pauling's type [6]. These simulations have shown that the spinel structure has a mixed character which ranges from normal to inverse spinel and depends on temperature. Molecular dynamics simulations have also been able to predict the thermodynamic evolution and spectroscopic perturbation of the catalytic system La<sub>2</sub>O<sub>3</sub>/γ-Al<sub>2</sub>O<sub>3</sub> [7].

In the present work a theoretical analysis of the structure and spectra of ZnAl<sub>2</sub>O<sub>4</sub> based on molecular dynamics simulations at 300 and 800 K is reported. The radial distribution functions and the vibrational spectra calculated from the molecular dynamics simulations are compared with experimental values. The Zn and Al environments in ZnAl<sub>2</sub>O<sub>4</sub> spinel are studied for both temperatures.

## 2. Experimental

Zinc aluminate was prepared by coprecipitating the corresponding nitrates (Baker 99 wt%) with ammonium carbonate. The precipitate was washed with demineralized water and calcined at 1073 K in air for 6 h. The synthesized zinc aluminate had a specific surface area of 20 m<sup>2</sup>/g and a pore volume of 0.15 ml/g as reported previously [4]. The pore size distribution in this preparation is bimodal and centered at  $D = 50$  Å and  $D = 180$  Å.

A Philips diffractometer (diffracted beam monochromator), coupled to a molybdenum anode X-ray tube, was used to obtain the diffractograms from  $2\theta = 6^\circ$  to  $110^\circ$ . The radial distribution functions were obtained using the Magini and Cabrini program [8].

Samples for infrared analysis were mixed with KBr and compacted to 16 mm disks under a load of 5 tons. The spectrometer was a FTIR Nicolet 170-SX.

## 3. Calculations

### 3.1. INTERACTION POTENTIAL

Molecular dynamics simulations involve the solution of the classical equations of motion of a set of  $N$  particles which interact through a pairwise additive potential. In our simulations a Pauling type function was used, which included a Coulombic term and a steric repulsion term given by

$$V(r_{ij}) = \frac{q_i q_j e^2}{r_{ij}} \left[ 1 + \text{sign}(q_i q_j) \left( \frac{\sigma_i + \sigma_j}{r_{ij}} \right)^n \right],$$

where  $r$  is the interatomic distance,  $q$  are the effective charges, and  $\sigma$  is the effective

Table 1  
Potential parameters

	$q(e)$	$\sigma(\text{\AA})$
Al	1.65	0.62
O	-1.10	1.20
Zn	1.10	0.74

ionic radius. The exponent  $n$  was taken to be 9 following Adams and McDonald [9]. The values of charges and ionic radii used in the simulations are the ones previously used [6,7] and are shown in table 1. Since the aluminum effective radius changes with coordination an average value was taken. The charges on aluminum and oxygen were taken from a previous work [6] where they were estimated from ab initio SCF-MO calculations on a set of relevant clusters [10].

### 3.2. MOLECULAR DYNAMICS SIMULATIONS

A set of molecular dynamics simulations in the microcanonical ensemble at 300 and 800 K was performed on the system  $\text{ZnAl}_2\text{O}_4$  spinel consisting of 432 aluminum atoms, 864 oxygen atoms, and 216 zinc atoms arranged in a cubic box with periodic boundaries (see fig. 1a). All zinc atoms were tetrahedrally coordinated [11] and all aluminum atoms were octahedrally coordinated at a density of  $4.6 \text{ g/cm}^3$ .

The original configuration in both cases was relaxed for 10 ps and the production stages were of 5 ps to calculate radial distribution and velocity autocorrelation functions. Vibrational spectra were calculated by Fourier transforming the autocorrelation functions. In both cases a time step  $\Delta t = 10^{-15} \text{ s}$  was used. The long range Coulombic potential was handled by the Ewald [12] method and the calculation of the corresponding forces was performed through spline interpolation and numerical derivatives. Energy fluctuations were at most 0.05% relative to the mean value.

## 4. Results and discussion

### 4.1. STRUCTURE

Fig. 2 shows the radial distribution function obtained from the X-ray diffraction data. This radial distribution was obtained at room temperature (300 K) on the zinc aluminate dried and calcined at 1073 K. This curve has to be interpreted in terms of fig. 3 where the theoretical radial distribution functions are shown. The locations of the first Al–O and Zn–O peaks are at 1.95 and 2.03 Å respectively, hence the first experimental peak found at 1.9 Å corresponds to these interatomic distances (see table 2). The estimated difference between Al–O and Zn–O (0.08 Å)

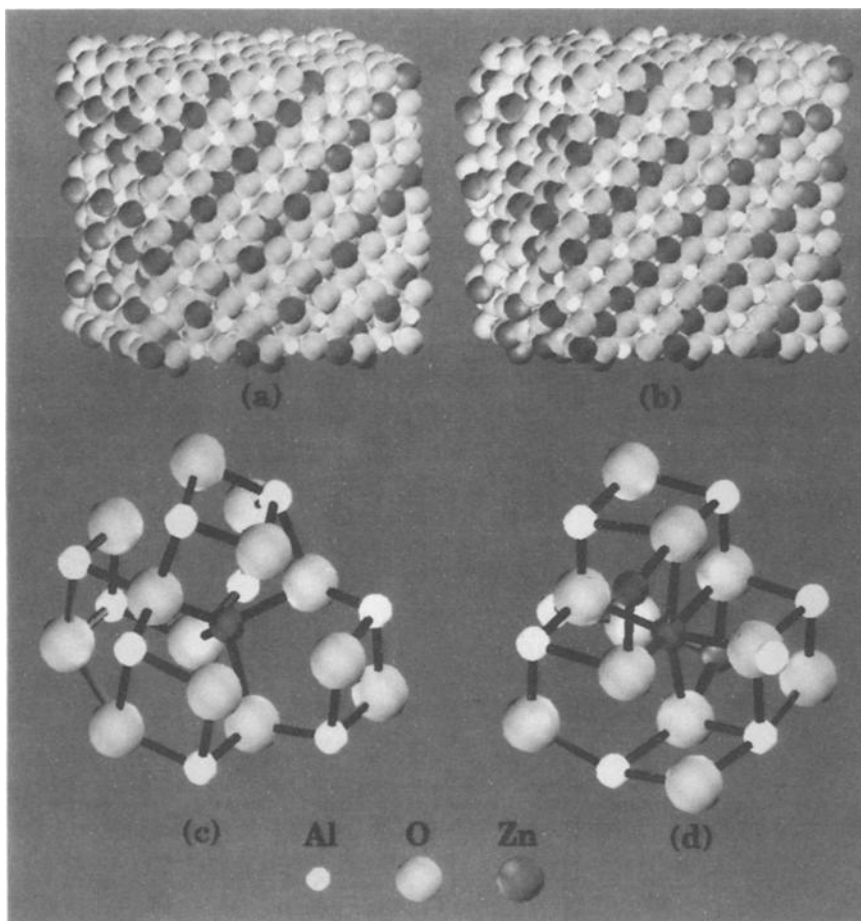


Fig. 1. (a) Snapshot of the configuration of  $\text{ZnAl}_2\text{O}_4$  used in the molecular dynamics simulations at 300 K after 15 ps; (b) snapshot of the configuration after 15 ps at 800 K; (c) local configuration of a zinc atom in a tetrahedral site at 300 K; (d) after increasing the temperature to 800 K, the same atom displaces 1.25 Å and occupies an octahedral site.

is not enough to be resolved experimentally. Again the difference between the locations of Al–Al, O–O and Al–Zn peaks (2.96, 2.64 and 2.98 Å) is too small to be resolved experimentally. Only a small shoulder is observed at 2.8 Å.

The sharp and broad experimental peak at 3.40 Å can be understood if the Al–Al, Al–O, Al–Zn and Zn–O distances are considered. Theoretically, these peaks are found at 3.49, 3.47, 3.88 3.45 and 2.68 Å respectively. These are second neighbor peaks and they are summarized in table 3. The O–O and Zn–O (3.88 and 3.68 Å) are low intensity peaks, and contribute only to the broadening of this experimental peak.

For the third neighbor peaks the experimental curve is apparently more struc-

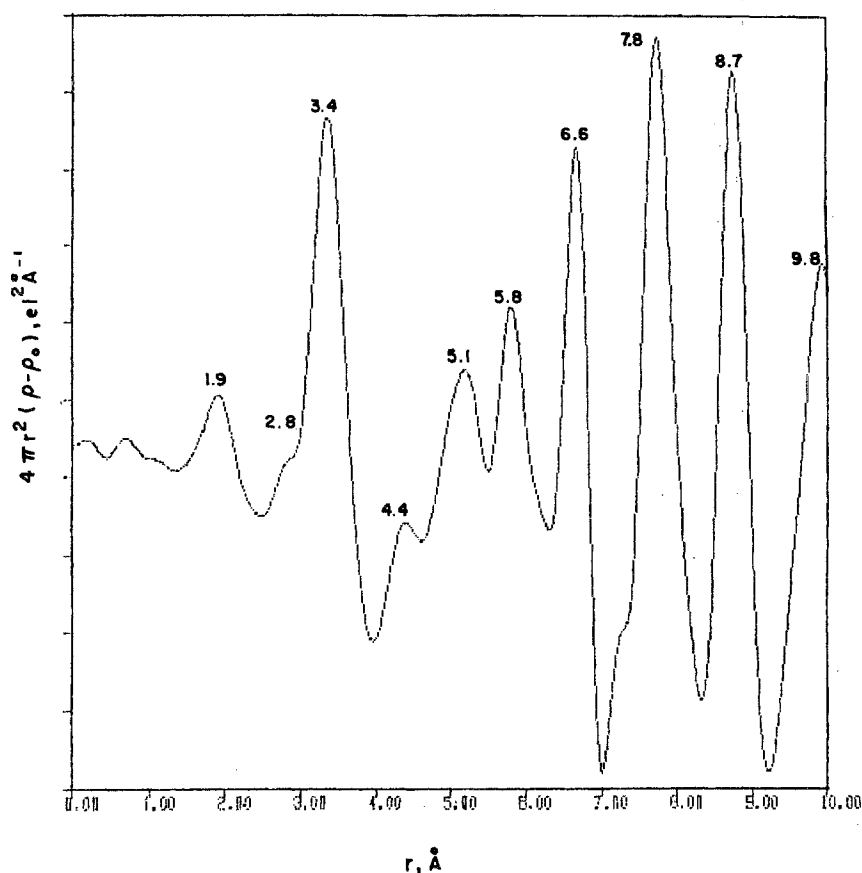


Fig. 2. Radial distribution function, obtained from the X-ray diffraction data at 300 K.

tured than the theoretical ones. The experimental radial distribution function is comparable to the weighted sum of the partial distribution functions. Therefore the larger the radii the larger the contribution to the sum. In table 3 the locations of experimental peaks found at distances larger than 4 Å are compared to those theoretically predicted.

To determine the effect of temperature on the structure, the same radial distribution functions were estimated at  $T = 800$  K (fig. 4). This is the temperature at which the spinel is used as catalyst support in dehydrogenation reactions [4,13]. All radial distribution functions are less structured than those obtained at  $T = 300$  K. In table 4 the positions of the first peak of the theoretical radial distribution functions at 300 and 800 K are compared

In the radial distribution functions at 800 K the features observed at 300 K are attenuated due to thermal vibration of particles. However, it can be observed that all interatomic distances are essentially the same for both temperatures (variations of around 2%) whereas the distance Zn–Zn increases by 6.4%.

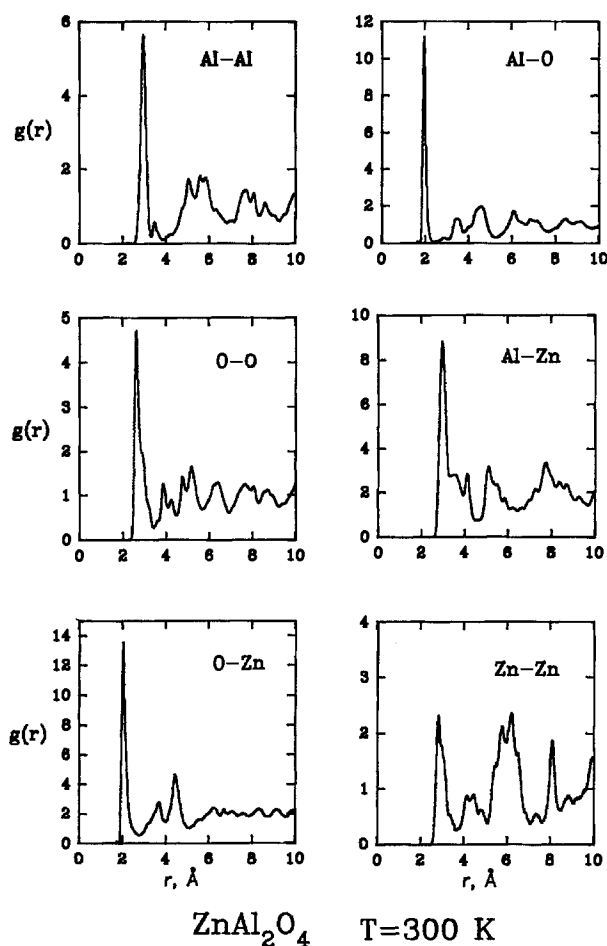


Fig. 3. Radial distribution functions calculated from the molecular dynamics simulations at 300 K.

At low temperature  $\text{Zn}^{2+}$  would be expected to be in tetrahedral sites and  $\text{Al}^{3+}$  in octahedral sites. Indeed  $\text{Al}^{3+}$  ions have higher valences and are able to bond to more oxygen ions. However, after the relaxation process is carried out by the mole-

Table 2

Experimental and theoretical positions of the radial distribution peaks of  $\text{ZnAl}_2\text{O}_4$  ( $R < 4.0 \text{ Å}$ )

Experimental values ( $\pm 0.3 \text{ Å}$ )	Theoretical values ( $T = 300 \text{ K}$ )					
	Al-Al	Al-O	O-O	Al-Zn	Zn-O	Zn-Zn
1.9		1.95			2.03	
2.8	2.96		2.64	2.98	2.80	
3.4	3.49	3.47		3.45	3.38	
				3.88		3.68

Table 3

Experimental and theoretical positions of the radial distribution peaks of  $\text{ZnAl}_2\text{O}_4$  ( $R \geq 4.0 \text{ \AA}$ )

Experimental values ( $\pm 0.3 \text{ \AA}$ )	Theoretical values ( $T = 300 \text{ K}$ )					
	Al-Al	Al-O	O-O	Al-Zn	Zn-O	Zn-Zn
4.4		4.62	4.25	4.14	4.44	4.44
5.1	5.07			5.10		4.84
5.8	5.59			5.54		5.76
6.6		6.13				6.38

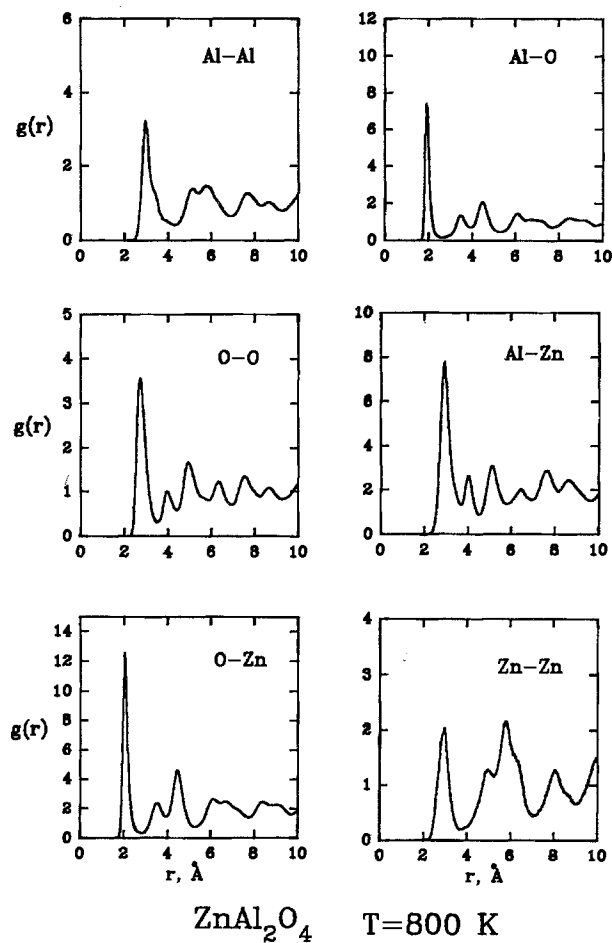


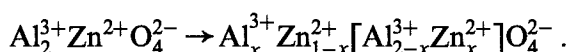
Fig. 4. Radial distribution functions calculated from the molecular dynamics simulations at 800 K.

Table 4

First peak positions of the radial distribution function of ZnAl<sub>2</sub>O<sub>4</sub> at  $T = 300$  K and  $T = 800$  K

	Theoretical positions of the first peak (Å)		
	300 K	800 K	(%)
Al–Al	2.96	2.96	0.0
Al–O	1.95	1.91	–2.0
O–O	2.64	2.69	+1.9
Al–Zn	2.98	2.91	–2.3
Zn–O	2.03	2.03	0.0
Zn–Zn	2.80	2.96	6.4

cular dynamics simulations at a constant temperature of 300 K, the perfect crystal structure is not totally preserved (see fig. 1b). Even at 300 K some tetrahedral sites are occupied by Al<sup>3+</sup> and the octahedral sites are shared by the divalent and trivalent ions. This process predicted by the molecular dynamics can be described by the following reaction:



The structure at 800 K tends towards a mixed spinel structure. This behavior has been observed for heavier ions such as lanthanum in the catalytic system La<sub>2</sub>O<sub>3</sub>/γ-Al<sub>2</sub>O<sub>3</sub>. Small displacements of Zn ions promote local crystallographic phase transitions and give rise to the mixed spinel structure, although this transformation could be due to the fact that we use an average value for the aluminum radius, because of the limitations of molecular dynamics simulations. In figs. 1c and 1d the typical environment of Zn ions is shown. Zn ions are originally four coordinated and after moving an average of 1.25 Å they become octahedrally coordinated. By careful inspection of figs. 1c and 1d, it seems that Zn ions move towards a nearby vacant octahedral site, generating a reordering of oxygen ions in the vicinity.

#### 4.2. SPECTRA

Fig. 5 shows the velocity vibrational spectrum obtained at room temperature on ZnAl<sub>2</sub>O<sub>4</sub> dried and calcined at 1073 K. The intense band at 3450 cm<sup>–1</sup> corresponds to adsorbed molecular water. Bands observed in the range 600–1400 cm<sup>–1</sup> are due to the various Al–O vibrations. Finally Zn–O vibrations are located at 505 and 562 cm<sup>–1</sup>.

Figs. 6 and 7 present the corresponding autocorrelation functions and the



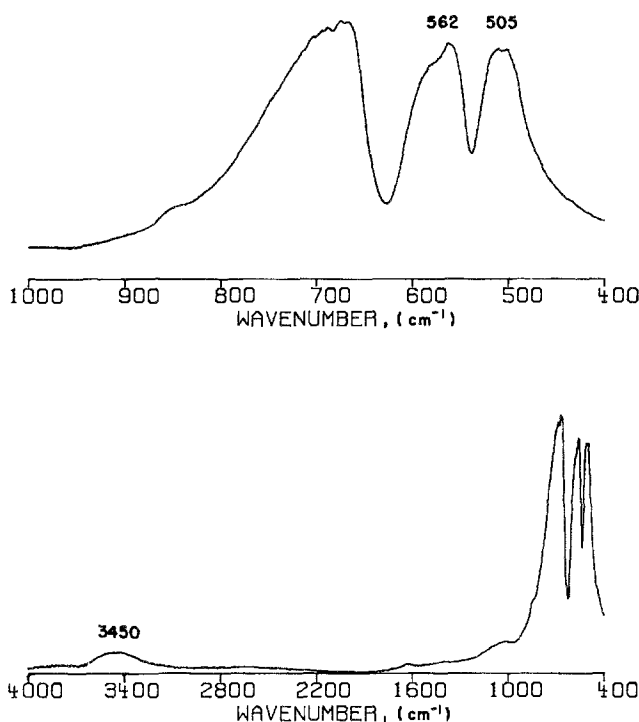


Fig. 5. Experimental infrared spectra.

vibrational spectra obtained by molecular dynamics at 300 and 800 K. The Al function is dominated by several oscillations, the most significant appear, after Fourier transformation, at frequencies of about 1000, 800 and 500  $\text{cm}^{-1}$ . The first two bands have been related to the Al–O stretch whereas the third is assigned to Al–O–Al bending vibrations. The power spectrum of oxygen shows a band from 950 to 1700  $\text{cm}^{-1}$  which has also been attributed to bending motions. In the case of Zn the peak is quite sharp and located at 400  $\text{cm}^{-1}$  but also two small peaks are found at 100 and 550  $\text{cm}^{-1}$  which agree fairly well with the experimental values. At 800 K the Al peaks are found in the same frequency interval but the spectrum is less structured and vibrations are less defined. The oxygen peak is also smoothed due to temperature effects. The Zn peak shows an oscillation not found at 300 K and is located at 400  $\text{cm}^{-1}$  (see table 5).

## 5. Conclusions

Radial distribution and velocity autocorrelation functions obtained from molecular dynamics simulations compare fairly well with the experimental data

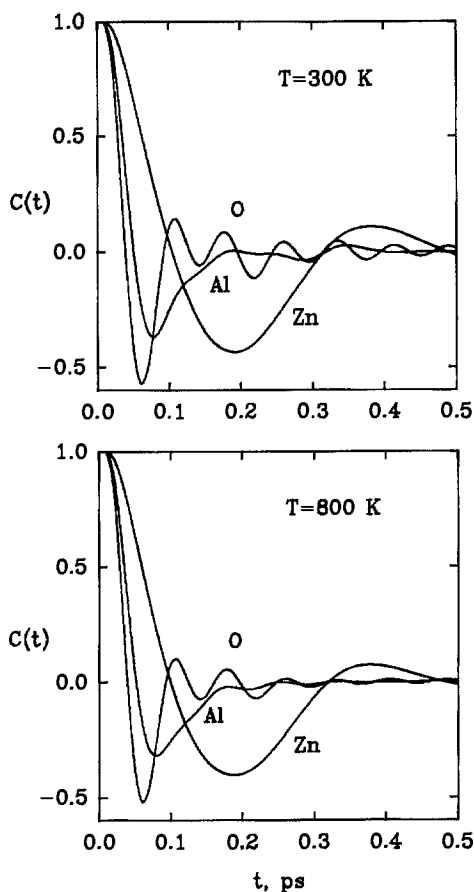


Fig. 6. Calculated autocorrelation functions at 300 and 800 K.

obtained and reported for  $\text{ZnAl}_2\text{O}_4$ . The theoretical results are richer in detail and allow a better interpretation of each experimental peak. Furthermore, a structural reinterpretation of the structure of  $\text{ZnAl}_2\text{O}_4$  spinel is envisaged as a mixed spinel structure as suggested by the theoretical studies of Grimes et al. [5], rather than a normal one [11] since simulations show small changes in the local environment around Zn ions. The detailed mechanism of this transformation will be described in a future work where the role of aluminum ionic radius will be thoroughly studied. Although, in some previous studies on alumina based compounds the influence of aluminum radius does not seem to be determining in the overall structural properties of the systems [6,7,14]. Based on these results for the bulk structure some considerations about the behavior of the surface can be made. The reconstruction of the surface should be expected to be a function of temperature. The surface ion positions after such a reconstruction could be interpreted as a disordered structure,

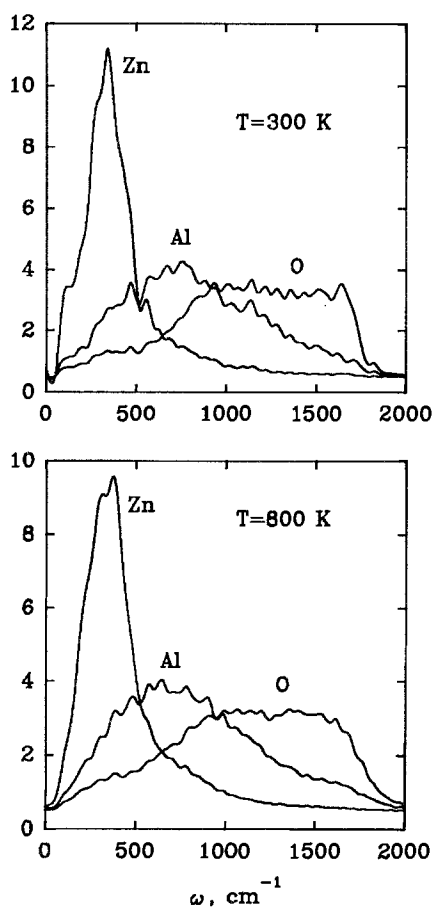


Fig. 7. Calculated vibrational spectra obtained by molecular dynamics at 300 and 800 K.

however the mixed nature of the spinel allows multiple coordinations of both aluminum and zinc ions in random positions, therefore appearing as a disordered structure.

Table 5

Experimental and theoretical spectral values ( $\text{cm}^{-1}$ ) at  $T = 300 \text{ K}$  and  $T = 800 \text{ K}$

Experimental	Theoretical	
	300 K	800 K
3450 ( $\text{H}_2\text{O}$ )		
600–1400 (Al–O)	500–1700 (Al)	500–1700 (Al)
505–562 (Zn–O)	450 (Zn)	400, 450 (Zn)

## Acknowledgement

This work was partially supported by Cray Research, Inc. under supercomputing grant DGAPASC-00192, UNAM (LJA).

## References

- [1] G.C. Bond, Chem. Soc. Rev. 20 (1991) 441.
- [2] J.T. Richardson, *Principles of Catalyst Development* (Plenum Press, New York, 1989).
- [3] T. Hutson Jr., US Patent 4,041,099 (1977).
- [4] M.A. Valenzuela, G. Aguilar, P. Bosch, G. Armendariz, P. Salas and A. Montoya, Catal. Lett. 15 (1992) 179.
- [5] R.W. Grimes, R.B. Anderson and A.H. Heuer, J. Am. Chem. Soc. 111 (1989) 1.
- [6] L.J. Alvarez, J. Fernández, M.J. Capitán and J.A. Odriozola, Chem. Phys. Lett. 192 (1992) 463.
- [7] L.J. Alvarez, J. Fernandez, M.J. Capitán and J.A. Odriozola, THEOCHEM, in press.
- [8] M. Magini and A. Cabrini, J. Appl. Cryst. 5 (1972) 14.
- [9] D.J. Adams and I.R. McDonald, Physica B 79 (1979) 159.
- [10] M.J. Capitán, M.A. Centeno, R. Alvero, J.J. Benítez, I. Carrizosa and J.A. Odriozola, in: *Proc. 12th Iber. Symp. of Catal.*, Vol. 2, Rio de Janeiro 1990, p. 250.
- [11] H.D. Megaw, *Crystal Structures, a Working Approach*, Studies in Physics and Chemistry, No. 10 (Saunders, New York, 1973).
- [12] M.P. Allen and D.J. Tildesley, *Computer Simulation of Liquids* (Clarendon Press, Oxford, 1989).
- [13] G. Aguilar Rios, M.A. Valenzuela, H. Armendáriz, P. Salas, J.M. Domínguez, D.R. Acosta and I. Schifter, Appl. Catal. A 90 (1992) 25.
- [14] L.J. Alvarez, J. Fernandez, M.J. Capitán and J.A. Odriozola, Catal. Lett. 21 (1993) 89.